RAPID COMMUNICATION

Room-temperature growth of high-quality ZnO nanocrystals using a dressed-photon-assisted near-field process

T. Yatsui · K. Nakanishi · K. Kitamura · M. Ohtsu

Abstract Single-crystalline ZnO nanocrystals were fabricated by room-temperature photo-chemical vapor deposition (PCVD). We further enhanced the growth of high-quality single-crystalline ZnO nanocrystals using dressed photons and phonons (DPPs). This resulted in greater position control and the growth of high-quality ZnO nanocrystals. The ZnO nanocrystals produced with DPPs had excellent cathodoluminescence characteristics, indicating that the near-field PCVD process could be a promising technique for nanophotonic integrated circuit production.

1 Introduction

Future optical transmission systems require nanometer-scale photonic devices (nanophotonic devices [1]) composed of quantum dots (QDs) to increase data transmission rates and capacity. One representative device studied by the authors is a nanophotonic switch [2, 3]. Recently, Kawazoe et al., succeeded in fabricating AND-gate and NOT-gate devices that operated at room temperature using InAs QD pairs [4], in which switching dynamics are controlled by a dipole-forbidden optical energy transfer among resonant energy levels in QDs via an optical near field.

To fabricate nanophotonic devices and their integrated circuits, QDs must be deposited on a substrate with nanoscale position control. To achieve this level of control,

we have demonstrated the feasibility of nanoscale chemical vapor deposition (CVD) by scanning a near-field fiber probe [5] as well as the deposition of 60-nm Zn dots with nanoscale control [6]. Although selective growth of semiconductor QDs via a self-assembly has recently been demonstrated by either metal catalyst-assisted [7, 8] or catalyst-free methods [9, 10], only limited semiconductor nanomaterials, substrates, and growth temperatures were used.

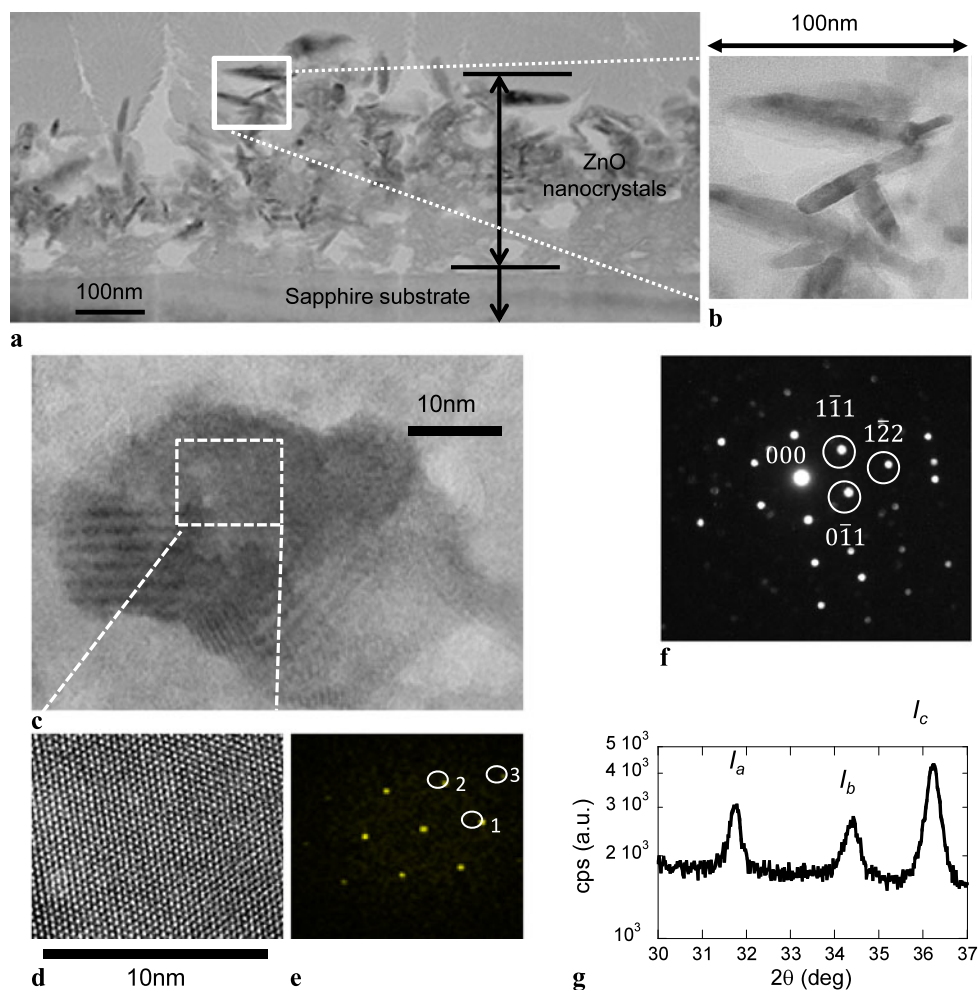## 2 Dressed-photon-assisted near-field process

To achieve greater position control, we used the optical near-field. The optical near-field is a virtual photon that couples with an excited electron. The quasiparticle representing this coupled state is called a dressed photon (DP) [11]. The energy of a dressed photon is larger than the energy of a free photon due to the contribution from coupling with the excited electron energy. In addition to excite electron coupling, the DP interacts with the crystal lattice structure of the nanomaterial by coupling with the multimodes of the phonons. As a result, the DP can dress the energy of phonons in a coherent state [12]. The coupled state of the DP and the coherent phonon (dressed photon and phonon or DPP) is a quasiparticle. The energy of the DPP is larger than that of the DP and the incident free photon, contributed from the electron and phonon. The use of DPPs has facilitated novel nanoscale technology [13, 14].

The ZnO nanocrystal is potentially ideal for room-temperature nanophotonic device production due to its high exciton-binding energy [15–17] and great oscillator strength [18]. For this reason, ZnO was used to demonstrate the feasibility of room-temperature nanocrystal growth by DPPs.

T. Yatsui (✉) · K. Nakanishi · K. Kitamura · M. Ohtsu
School of Engineering, University of Tokyo, Bunkyo-ku, Tokyo, 113-8656, Japan
e-mail: yatsui@ee.t.u-tokyo.ac.jp

T. Yatsui · M. Ohtsu
The Nanophotonics Research Center, University of Tokyo, Bunkyo-ku, Tokyo, 113-8656, Japan

Fig. 1 (**a**) TEM image of the ZnO nanocrystals deposited on a sapphire substrate. (**b**) Magnified TEM image in the area indicated by the white open square in (**a**). (**c**) and (**d**) high-resolution TEM images. (**e**) FFT image of (**d**). (**f**) The selection area diffraction (SAD) pattern of (**d**) taken from the (011) direction. (**g**) XRD θ–2θ scan result of (**a**)

# 3 Room temperature growth of ZnO nanocrystal using photochemical vapor deposition

ZnO nanocrystals grown using photochemical vapor deposition (PCVD). PCVD reduces the growth temperature by producing reactive radicals via the photolysis of their precursors [19]. As a result, higher position alignment can be realized due to the reduction in the thermal diffusion of the nanoparticles deposited on the substrate.

As a preliminary study of the position selective growth of nanocrystals by DPPs, we carried out conventional PCVD for ZnO nanocrystal growth. Diethyl zinc (DEZn) and oxygen were used as II and VI sources. Argon was used as the carrier gas for DEZn. The II/VI ratio was 9/20,000. The total pressure in the reaction chamber was 5.0 Torr. Q-switch pulsed laser light (5.82 eV, λ = 213 nm, 20 Hz, pulse width = 5 ns) was used as the light source for PCVD growth. The photon energy of the light source exceeds the absorption band-edge energy of DEZn (4.59 eV) [20]. The growth time was 3 hours.

Low-magnification transmission electron microscopy (TEM), shown in Figs. 1(a) and 1(b), revealed rod-shaped structures with 50–100 nm in length and 5–10 nm in diameter. High-resolution TEM images (Figs. 1(c) and 1(d)) and the corresponding fast Fourier transform (FFT) pattern (Fig. 1(e)) revealed a periodic structure indicating single-crystalline formation. Using inverse FFT, we determined that the lattice spacing (0.280, 0280, 0.163 nm) matched the ZnO wurtzite planes; 0.284 nm along the (100) plane, 0.281 nm along the (010) plane, and 0.165 nm along the (110) plane. From these results, the TEM images of Figs. 1(c) and 1(d) are of the wurtzite ZnO crystal from the (001) direction. These results were also confirmed by selection area diffraction (SAD) patterns obtained from the (011) direction (Fig. 1(f)), where the selective spot indicated by the white open circles matched the lattice spacing of wurtzite ZnO $(1\bar{1}1)$, $(1\bar{2}2)$, and $(0\bar{1}1)$. The X-ray diffraction (XRD) θ–2θ scans, shown in Fig. 1(g), indicate three peaks at 31.77 (I_a), 34.42 (I_b), and 36.25 (I_c) degrees, corresponding to ZnO (100), ZnO (001), and ZnO (101), respectively. These results confirm that the obtained structure

Fig. 2 (**a**) Temperature-dependent PL spectra of deposited ZnO nanocrystals. (**b**) Room-temperature (300 K) PL spectrum. (**c**) Temperature dependence of the emission peak energy. *Solid lines* show the calculated temperature-dependent PL peak position using Varshni's equation
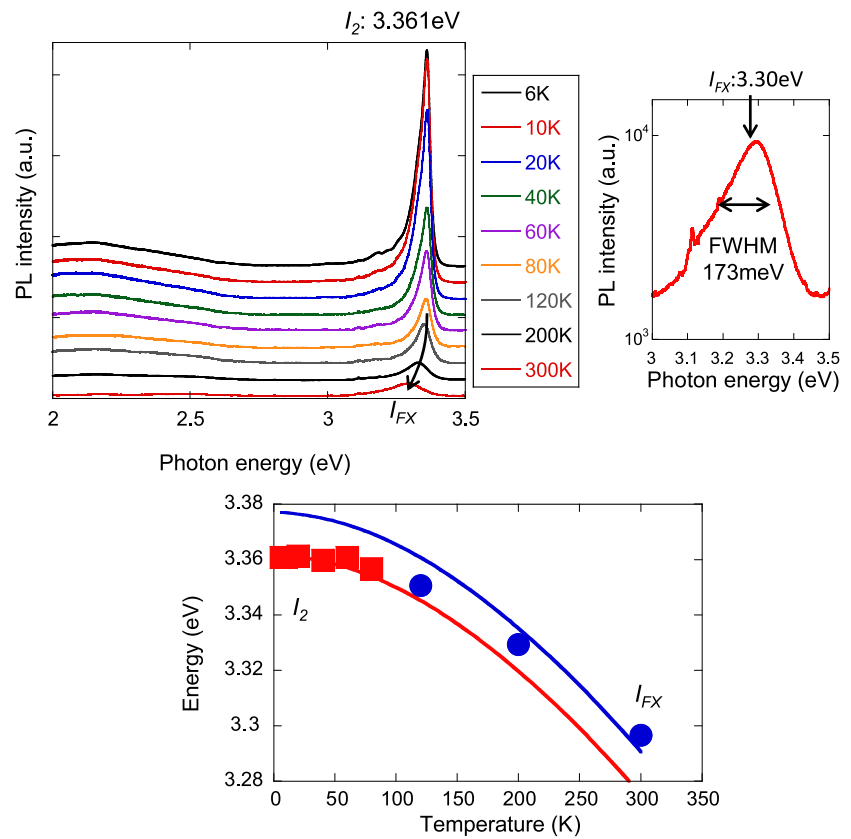
was a wurtzite ZnO single crystal and deposited with random direction with respective to the substrate.

Photoluminescence (PL) was used to evaluate the optical properties of the deposited nanocrystals. We used a continuous-wave He–Cd laser ($\lambda = 325$ nm) as the excitation light source. The temperature-dependent PL spectrum (Fig. 2(a)) shows a strong sharp peak at 3.361 eV (I_2) at 6 K. This PL peak originates from the bound exciton in wurtzite ZnO [18]. As the temperature increased, the PL intensity of this peak decreased dramatically. In addition, a new peak (labeled I_{FX}) emerged at temperatures above 100 K; I_{FX} remained visible even at room temperature. Figure 2(b) shows the magnified PL spectrum at room temperature (300 K) with a sharp peak at 3.30 eV. Its full width at half maximum (FWHM) is 173 meV, which is comparable to that of a single-crystalline ZnO nanorod (158 meV) grown by metal-organic vapor phase epitaxy (MOVPE) under 450 °C high-growth temperature conditions [21]. These characteristics presumably resulted from the recombination of the neutral donor-bound exciton to the free exciton in wurtzite ZnO. The temperature dependence of the energy at the peaks I_2 and I_{FX} is fitted using Varshni's equation (solid curves in Fig. 2(c)) [22], which defines the temperature dependence of the band gap. These results indicated that the ZnO nanocrystals synthesized by PCVD at room temperature were as high

quality as the ZnO synthesized using MOVPE with a high growth temperature of 450 °C.

4 Room temperature growth of ZnO nanocrystal using dressed-photon-assisted near-field process

Based on the experimental results of the conventional PCVD described above, we proceeded to grow ZnO nanocrystals at room temperature using the DPP process. To generate DPPs, a patterned substrate with 200-nm-diameter holes and a 400-nm center-to-center period was fabricated on a 40-nm-thick SiO_2 film (Fig. 3(a)). A Q-switched pulsed laser with lower energy (3.49 eV, $\lambda = 355$ nm, 20 Hz, pulse width = 5 ns) was used to prevent DEZn dissociation at the free space. DEZn can be selectively dissociated at the pattern edge by the DPP (Fig. 3(b)). Although no nanoparticles were deposited after 10-minute gas flow without irradiation (Fig. 3(c)), the deposition of nanoparticles at the rim of the hole (indicated by the white arrows) was confirmed after 10-minute gas flow with light irradiation of 3.49-eV (Fig. 3(d)). The nanoparticle deposition sites were sparse, despite the fact that the spot irradiated by the 3.49-eV light source was 1 mm in diameter. We evaluated the distance d between the nearest edge of the 100-nm hole and the nanoparticle center. The shapes of the nanoparticles were approximated by

Fig. 3 (**a**) SEM image of the hole array substrate. (**b**) Schematic of ZnO-nanocrystal deposition using a DPP. SEM images the substrate after (**c**) 10-minutes without irradiation and (**d**) 10-minutes with irradiation. (**e**) Histogram of the obtained distance d. (*Inset*: schematic of the distance d between the nearest edge of the hole and the center of the nanoparticle)
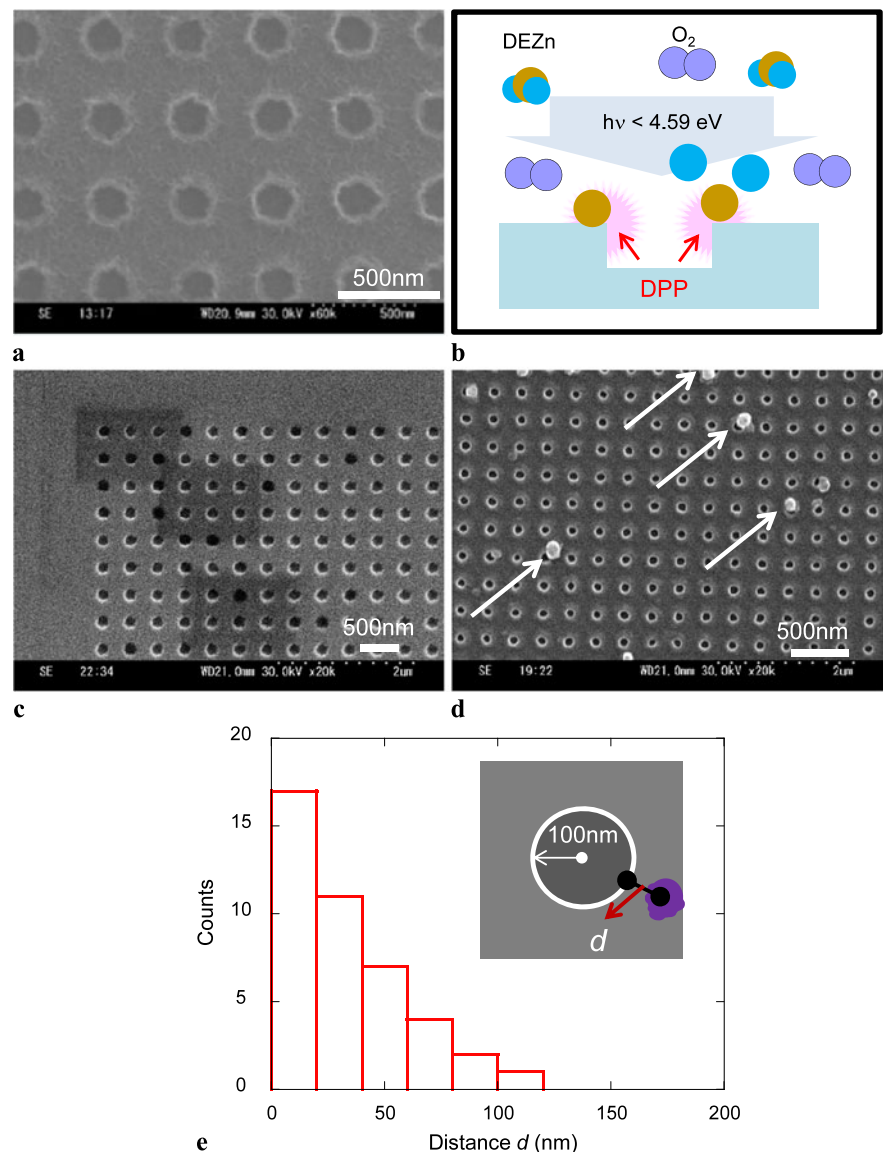
circles of equal area. Figure 3(e) shows the histogram of d. From this result, 40-% of the nanoparticles were deposited within 20 nm of the edge, indicating that deposition was realized by DPPs generated at the rim of the hole structure. The results have shown the potential of DPPs for higher position-selective alignment.

We used cathodoluminescence (CL) to evaluate the optical properties of the deposited nanoparticles. Figures 4(a) and 4(b) show the scanning electron microscopy (SEM) image of the deposited nanoparticles and the corresponding CL mapping at 3.36 eV taken at 93 K, which corresponds to the energy of the free exciton emission peak of wurtzite ZnO nanocrystals (blue solid curve in Fig. 4(c)). In addition, the room-temperature CL spectrum has a high peak at 3.29 eV with a width of 140-meV (red solid curve in Fig. 4(c)), which is comparable to that fabricated using MOVPE un-

der high growth temperature (450 °C). From these results, we confirmed that the deposited nanoparticles were high-quality wurtzite ZnO.

5 Conclusion

The use of PCVD allowed room-temperature growth of single-crystalline ZnO nanocrystals. Additionally, using a DPsP generated in the nanoscale structure, we realized room-temperature growth of high-quality ZnO nanocrystals. We confirmed their excellent CL characteristics at room temperature. Because the deposition technique uses a photochemical reaction at room temperature, it can be applied to other materials and other substrates.

Fig. 4 (**a**) Typical SEM image of the deposited ZnO nanocrystal and (**b**) the corresponding CL image at 3.36 eV obtained at 93 K. (**c**) CL spectra obtained at 93 K (*blue solid curve*) and 300 K (*red solid curve*)
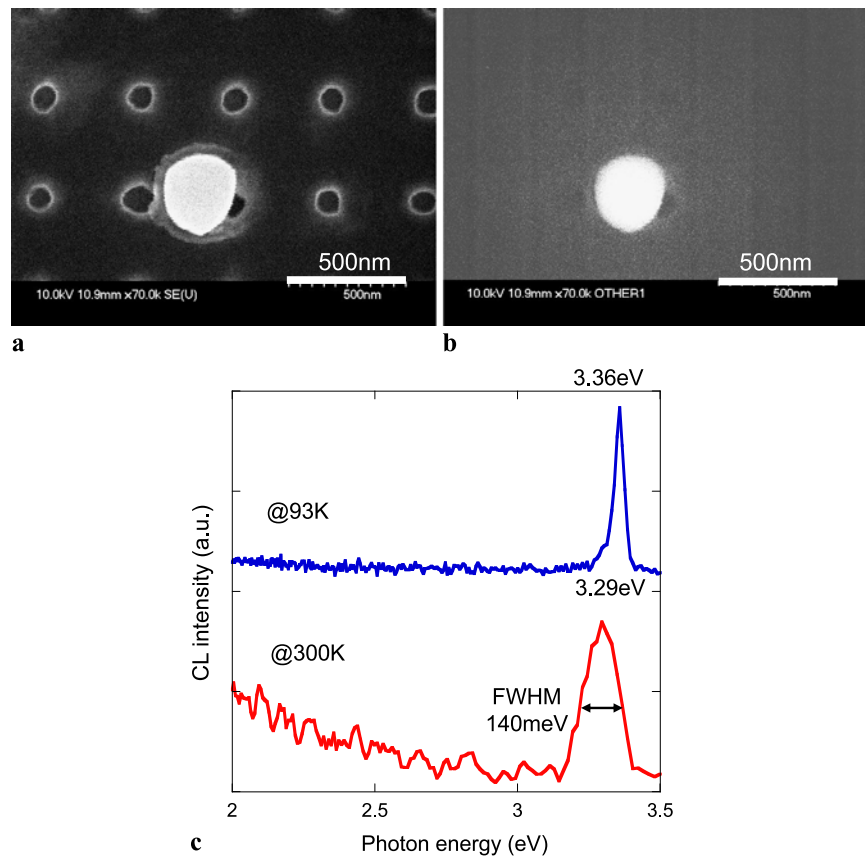
References

1. M. Ohtsu, T. Kawazoe, T. Yatsui, M. Naruse, IEEE J. Sel. Top. Quantum Electron. **14**, 1404 (2008)
2. T. Kawazoe, K. Kobayashi, S. Sangu, M. Ohtsu, Appl. Phys. Lett. **82**, 2957 (2003)
3. T. Yatsui, S. Sangu, T. Kawazoe, M. Ohtsu, S.J. An, J. Yoo, G.C. Yi, Appl. Phys. Lett. **90**, 223110 (2007)
4. T. Kawazoe, M. Ohtsu, S. Aso, Y. Sawado, Y. Hosoda, K. Yoshizawa, K. Akahane, N. Yamamoto, M. Naruse, Appl. Phys. B **103**, 537 (2011)
5. T. Yatsui, S. Takubo, J. Lim, W. Nomura, M. Kourogi, M. Ohtsu, Appl. Phys. Lett. **83**, 1716 (2003)
6. J. Lim, T. Yatsui, M. Ohtsu, IEICE Trans. Electron. **E88c**, 1832 (2005)
7. L.E. Jensen, M.T. Bjork, S. Jeppesen, A.I. Persson, B.J. Ohlsson, L. Samuelson, Nano Lett. **4**, 1961 (2004)
8. A.I. Hochbaum, R. Fan, R.R. He, P.D. Yang, Nano Lett. **5**, 457 (2005)
9. J. Noborisaka, J. Motohisa, T. Fukui, Appl. Phys. Lett. **86**, 213102 (2005)
10. S.D. Hersee, X.Y. Sun, X.T. Wang, Nano Lett. **6**, 1808 (2006)
11. K. Kobayashi, S. Sangu, H. Ito, M. Ohtsu, Phys. Rev. A **63**, 013806 (2001)
12. A. Sato, Y. Tanaka, F. Minami, K. Kobayashi, J. Lumin. **129**, 1718 (2009)
13. T. Yatsui, K. Hirata, W. Nomura, Y. Tabata, M. Ohtsu, Appl. Phys. B **93**, 55 (2008)
14. T. Kawazoe, T. Takahashi, M. Ohtsu, Appl. Phys. B **98**, 5 (2010)
15. A. Ohtomo, K. Tamura, M. Kawasaki, T. Makino, Y. Segawa, Z.K. Tang, G.K.L. Wong, Y. Matsumoto, H. Koinuma, Appl. Phys. Lett. **77**, 2204 (2000)
16. M.H. Huang, S. Mao, H. Feick, H.Q. Yan, Y.Y. Wu, H. Kind, E. Weber, R. Russo, P.D. Yang, Science **292**, 1897 (2001)
17. H.D. Sun, T. Makino, Y. Segawa, M. Kawasaki, A. Ohtomo, K. Tamura, H. Koinuma, J. Appl. Phys. **91**, 1993 (2002)
18. D.C. Reynolds, D.C. Look, B. Jogai, C.W. Litton, G. Cantwell, W.C. Harsch, Phys. Rev. B **60**, 2340 (1999)
19. S. Yamazaki, T. Yatsui, M. Ohtsu, Appl. Phys. Express **1**, 061102 (2008)
20. R.R. Krchnavek, H.H. Gilgen, J.C. Chen, P.S. Shaw, T.J. Licata, R.M. Osgood, J. Vac. Sci. Technol. B **5**, 20 (1987)
21. K. Kitamura, T. Yatsui, M. Ohtsu, G.C. Yi, Nanotechnology **19**, 175305 (2008)
22. Y.P. Varshni, Physica **34**, 149 (1967)